# A Pipeline from Non-invasive Imaging to Patient-Specific Models of Cardiac Electromechanics: An Atlas-based Approach

Matthew J. Gonzales[1], Gregory Sturgeon[2], W. Paul Segars[2], and Andrew D. McCulloch[1,3,4]

[1] Department of Bioengineering, University of California San Diego, La Jolla, CA, USA
{mjgonzales, amcculloch}@ucsd.edu

[2] Carl E. Ravin Advanced Imaging Laboratories, Duke University, Durham, NC, USA
{greg.sturgeon, paul.segars}@duke.edu

[3] Department of Medicine (Cardiology), University of California San Diego, La Jolla, CA, USA

[4] Cardiac Biomedical Science and Engineering Center, University of California San Diego, La Jolla, CA, USA

**Abstract.** We present a pipeline for constructing quadrilateral and hexahedral cardiac meshes from non-invasive imaging data suitable for simulations of cardiac electrophysiology and biomechanics. We use the software Blender to execute mesh improvement schemes, and to permit manual mesh improvement by a user interactively. Here, we present resulting meshes from one patient with near-isotropic elements, with uniform element size, and with regular angles. These meshes can be included in an atlas, and can be deformed to imaging data of another patient whose great vessels and pulmonary veins have identical topologies.

**Keywords:** patient-specific, cardiac meshes, mesh improvement, finite elements, electrophysiology

## 1 Introduction

Construction of high-quality cardiac meshes suitable for simulations of cardiac electrophysiology and biomechanics remains challenging, especially when the meshes are constructed from non-invasive imaging studies. Quadrilateral and hexahedral meshes customarily are more structured than simplicial meshes, adding an additional challenge to meshing. Though construction of a high-quality quadrilateral or hexahedral mesh can be tedious and lengthy, the topological simplicity of these meshes makes them easier to re-use as a template for new models compared with simplicial meshes.

Here, we describe a pipeline for constructing patient-specific cardiac meshes from non-invasive imaging studies. Our approach is guided by two points: First, since we plan on creating a small number of high-quality template meshes that may be de-

adfa, p. 1, 2011.

formed to new patient data, we do not require every step to be automatic. Second, we require our mesh improvement techniques to be implemented in an interactive environment; this way, any limitations of the mesh improvement techniques can be detected and fixed manually. We use the software Blender (http://www.blender.org/) as an interactive environment because it has some native meshing tools and is scriptable in Python (http://www.python.org/). Computationally intensive steps may be completed using the NumPy extension of Python (http://numpy.scipy.org/). Using these tools, we can construct models of the heart with quality sufficient for finite element simulations of biomechanics and electrophysiology.

## 2 Methods

### 2.1 Imaging and Segmentation

A 68-year old male with atrial fibrillation underwent a computed tomography (CT) study (General Electric 64-slice Lightspeed CT Scanner, 0.5x0.5x0.625 mm) with electrocardiogram gating as part of an Institutional Review Board-approved research study after giving informed consent. The four cardiac chambers and valve apparatuses were segmented and triangulated by a marching cubes algorithm implemented in ITK-SNAP (http://www.itk-snap.org/) [1].

### 2.2 Interactive Construction of Topology

We constructed quadrilateral and hexahedral meshes of the left atrium (**Figure 1A**) and right atrium comprising sub-regions with regular, grid topologies (i.e., parametric coordinates were preserved between adjacent elements). Extraordinary vertices (verti-

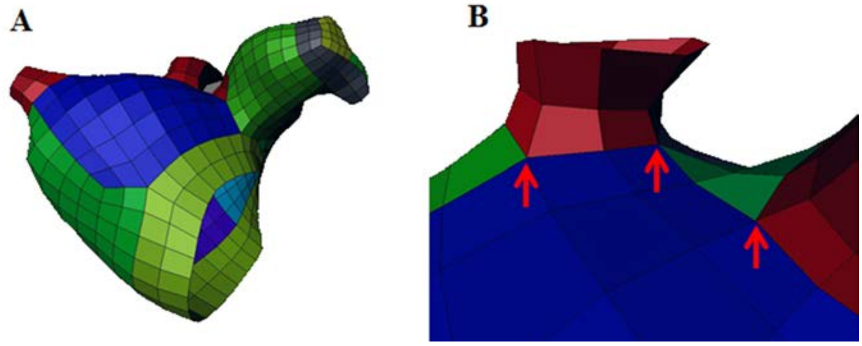


**Fig. 1.** (**A**) An anterior view of the left atrial endocardium discretized into quadrilaterals. Colors denote sub-regions each having local "grid" topologies. (**B**) Topology regions are separated by irregular (extraordinary) vertices (arrows), each with five connected neighbors rather than the regular four, at regions of high curvature.

ces with an irregular number of neighbors) were placed by trial and error, but the meshes had near-rectangular angles throughout when extraordinary vertices lay near regions of sharp curvature (e.g., the pulmonary veins; **Figure 1B**).

### 2.3 Interactive Optimization of Element Size and Shape

To improve element size uniformity, isotropy, and element angles of surface meshes, the scheme of Ohtake et al. [2] was used in concert with "one-to-four" subdivision [3] and with manual insertion of edge loops (Figure 2A). Application of edge loops followed by element regularization by the Ohtake scheme improved element size uniformity (Figure 2B). If the mesh topology is constructed with care, edge loops can be inserted at most locations in the mesh to improve the homogeneity of size. Other schemes were useful in the construction of hexahedral meshes [4].

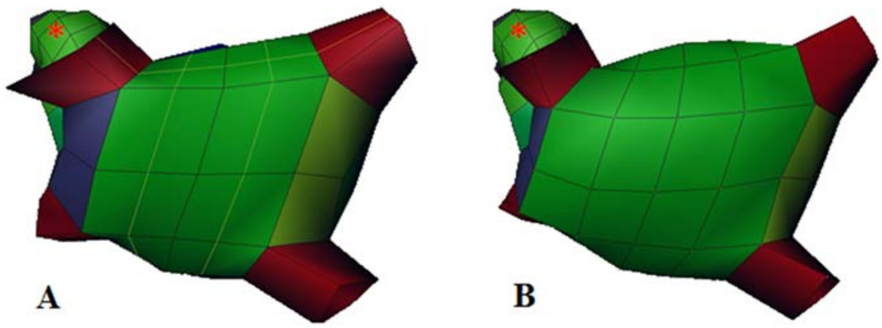


**Fig. 2.** Optimization of element shape and size using a combination of manual edge loop insertion and automatic regularization. Uniform subdivision (not shown) cannot improve element size uniformity, yet the left atrial appendage (asterisks) requires smaller elements to capture geometric detail at the coarsest mesh resolutions. In (**A**), edge loops (highlighted) are inserted in the posterior left atrial wall to decrease the size of the largest mesh quadrilaterals. In (**B**), the result of optimization by the scheme of Otake et al. [2] is displayed. The quadrilaterals are isotropic, have regular angles, have uniform sizes, and are closer in size to the quadrilaterals of the left atrial appendage.

## 3 Results

### 3.1 Mesh Statistics

We constructed coarse quadrilateral surface meshes of the left atrium (LA) and right atrium (RA) that captured their major geometric features; we name these LA-170 and RA-80, where the numeral indicates the number of quadrilaterals. Using edge loop insertion, a one-to-four subdivision [3], and the surface regularization scheme of

Ohtake et al. [2], we decreased the anisotropy ratio of the quadrilaterals, and decreased the coefficients of variation of the areas, anisotropy ratios, and angles of the quadrilaterals.

**Table 1.** Areas, anisotropy ratios, and angles of coarse meshes (LA-170, RA-80) and refined meshes (LA-4524, RA-4829). Values are presented as means, and coefficients of variation (parentheses). LA = Left atrium; RA = Right atrium.

| | LA-170 | LA-4524 | RA-80 | RA-4829 |
|---|---|---|---|---|
| Area ($mm^2$) | 95.7 (51) | 3.8 (43) | 219 (51) | 3.9 (44) |
| Anisotropy Ratio | 1.30 (23) | 1.26 (16) | 1.32 (24) | 1.31 (20) |
| Angle (degrees) | 88.5 (17) | 89.9 (14) | 90.6 (21) | 89.9 (17) |

### 3.2 Finite Element Simulations

We solved the monodomain equation to demonstrate the use of our meshes in a finite element problem. Degree of convergence was similar in different areas of the mesh because of the uniformity of element sizes, and quality of hexahedrals, as determined by aspect ratio (anisotropy) and by regularity of angles. Two images of a traveling wave on our patient-specific mesh are displayed in **Figure 3**.

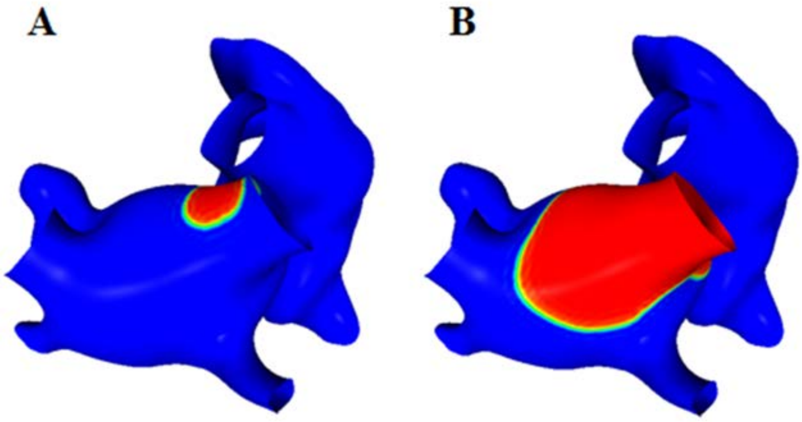


**Fig. 3.** A stimulus is applied at a pulmonary vein of the left atrium (**A**) and propagates on the posterior left atrial wall towards the remainder of the left atrial chamber and the right atrium (**B**). The electrical wave does not propagate centrifugally owing to anisotropic conductivity. Red areas are electrically active and blue areas are electrically inactive.

# 4 Discussion

## 4.1 Cardiac Atlas in Patient-specific Model Construction

Automatic methods place extraordinary vertices in a surface at critical points of Gaussian curvature, and construct sub-domains in accordance with the principal directions of curvature [5]. Nonetheless, these approaches rely on trial and error with user-defined parameters, and may be sensitive to image noise in unpredictable ways. In contrast, we place extraordinary vertices manually and optimize geometric accuracy, element angles, element isotropy, and element size uniformity according to the final application of the meshes.

A cardiac mesh for a new patient can be constructed easily if the size and topology of the heart are sufficiently similar to an existing template in the atlas, as we have shown previously [6]. If the heart of the new patient is dissimilar to all templates in the atlas, its topology can be constructed manually and added to the atlas.

## 4.2 Element Quality Effects on Cardiac Simulations

The condition number of a finite element problem is increased by non-uniform element sizes and elements with poor angle quality. Higher condition numbers increase solution error and adversely affect simulation time if an iterative solver, such as the biconjugate gradient method, is used. Element anisotropy may decrease simulation time and decrease solution error in biomechanics problems, owing to directional differences in strain gradients. In contrast, isotropy decreases solution time and decreases solution error in electrophysiology problems, because gradients of potential with similar magnitudes may arise in any direction, depending on the orientation of the traveling wave. Thus, the atlas provides a means to select a template mesh best-suited for an electrophysiology problem or a biomechanics problem, and further, to select a template mesh compatible with the desired solution accuracy and time constraints.

# 5 Conclusion

We demonstrate construction of patient-specific quadrilateral and hexahedral cardiac models with quality sufficient for finite element simulations. Automatic methods were used to optimize element shape and size, but manual construction and modification of mesh topology resulted in meshes further optimized for solution error and simulation time. These meshes can be incorporated into an atlas for deformable registration to the imaging data of another patient.

## References


1. Yushkevich, P.A., Piven, J., Hazlett, H.C., Smith, R.G., Ho, S., Gee, J.C., Gerig, G.: User-guided 3D active contour segmentation of anatomical structures: Significantly improved efficiency and reliability. Neuroimage. 31(3), 1116-1128 (2006)
2. Ohtake, Y., Belyaev, A.G., Bogaevski, I.A.: Polyhedral surface smoothing with simultaneous mesh regularization, In: Martin, R., Wang, W. (Eds.), Geometric Modeling and Processing, Hong Kong, pp. 229-237 (2000)
3. Li, G., Ma, W., Bao, H.: A new interpolatory subdivision for quadrilateral meshes. Comput. Graph. Forum. 24, 3-16 (2005)
4. Zhang, Y., Bajaj, C., Xu, G.: Surface Smoothing and Quality Improvement of Quadrilateral/Hexahedral Meshes with Geometric Flow. Commun. Numer. Meth. En., 25, 1-18 (2007)
5. Alliez, P., Cohen-Steiner, D., Devillers, O., Lévy, B., Desbrun, M.: Anisotropic polygonal remeshing. ACM T. Graphic. 22(3), 485-493 (2003)
6. Zhang, Y., Liang, X., Ma, J., Jing, Y., Gonzales, M.J., Villongco, C., Frank, L.R., Nigam, V., Stark, P., Narayan, S.M., McCulloch, A.D.: An Atlas-Based Geometry Pipeline for Cardiac Hermite Model Construction and Diffusion Tensor Reorientation. Med. Image Anal. DOI: 10.1016/j.media.2012.1006.1005 (2012)